

Nucleon-nucleus scattering as a test of shell structure of some light mass exotic nuclei

S. Karataglidis*

*Department of Physics and Electronics, Rhodes University,
P.O. Box 94, Grahamstown, 6140, South Africa.*

Y. J. Kim†

Department of Physics, Cheju National University, Jeju 690-756, Republic of Korea.

K. Amos‡

School of Physics, University of Melbourne, Victoria 3010, Australia

(Dated: March 11, 2018)

Abstract

Shell model wave functions have been used to form microscopic g -folding optical potentials with which elastic scattering data from ^8He , $^{10,11}\text{C}$, and $^{18,20,22}\text{O}$ scattering on hydrogen have been analyzed. Those potentials, the effective two-nucleon interaction used in their formation, and the shell model details, then have been used in distorted wave approximation calculations of differential cross sections from inelastic scattering to the first excited states of five of those radioactive ions.

PACS numbers: 21.10.Hw,25.30.Dh,25.40.Ep,25.80.Ek

*Electronic address: S.Karataglidis@ru.ac.za

†Electronic address: yjkim@cheju.ac.kr

‡Electronic address: amos@physics.unimelb.edu.au

I. INTRODUCTION

Microscopic descriptions of exotic nuclei are becoming more important in the light of recent experiments involving the scattering of radioactive ion beams (RIBs) off hydrogen. In inverse kinematics, such equate to scattering of protons from the ions, and with current methods of analysis [1] of such scattering, a most complete map of their matter densities can be made. Such well tested descriptions of exotic nuclei will be of relevance in analyses of data to be taken with proposed electron-ion collider being built at GSI [2], as well as from the SCRIT project at RIKEN [3]. Descriptions of the charge densities, especially of nuclei with neutron halos, will require detailed microscopic models to account for the structure of the core.

Traditionally proton scattering has been one of, if not, the best means by which the matter densities of the nucleus may be studied. Microscopic models now exist that can predict results of both elastic and inelastic scattering reactions. When good, detailed specification of the nucleon structure of the nucleus is used, those predictions usually agree very well with observation, both in shape and magnitude. To facilitate such analyses of data, one first must specify the nucleon-nucleus (NA) interaction. To do so requires two main ingredients: a) an effective nucleon-nucleon (NN) interaction in-medium, allowing for the mean field as well as Pauli-blocking effects; and b) a credible model of structure for the nucleus that is nucleon-based. When the effective NN interaction is folded with the one-body density matrix elements (OBDM) of the target ground state, a microscopic NA interaction results. Such interactions have been used successfully in studies of the structures of stable nuclei (see [1] for a complete review of those studies), as well as of exotic nuclei [4, 5].

Herein, we consider the scattering of the exotic nuclei ${}^8\text{He}$, ${}^{10,11}\text{C}$, and ${}^{18,20,22}\text{O}$ from hydrogen, for which there are recent data. The data for the elastic scattering of ${}^8\text{He}$ from hydrogen at 15.7A MeV [6] was analyzed in terms of the JLM model using G matrix shell model wave functions of Navrátil and Barrett [7], as well as a coupled-channels model involving coupling to the ${}^8\text{He}(p,d){}^7\text{He}$ channel. Their analyses indicated a strong coupling to the (p,d) channel. This is problematic as ${}^7\text{He}$ is unbound. Any possible recoupling to reform ${}^8\text{He}$ in its ground state is highly unlikely. Indeed, their analysis based on this coupling required a scale strength of the imaginary part of the JLM potential of 0.2, which the authors attributed to compound nucleus effects. For ${}^8\text{He}$, the energy (15.7 MeV) lies well in its continuum and compound nucleus contribution to the elastic scattering is not likely to be that large. So such a sizable reduction in the imaginary part of the JLM optical potential seems to be unrealistic.

The JLM interaction was also used in the analyses of the scattering of the C [8] and O isotopes [9, 10] from hydrogen. For the analyses of the data from the C isotopes, and from ${}^{18,20}\text{O}$ the JLM potential was again used with the adjustment of parameters to fit the data. In the case of ${}^{22}\text{O}$ [9], two analyses were made: a) one using a folding model producing a real microscopic optical potential, but for which the imaginary part was obtained from a global phenomenological parameterization; and b) one using the JLM potential for which the neutron transition densities were adjusted to fit the data. As a consequence, those analyses may not necessarily be sensitive tests of the structures of the targets as any possible problems may be masked by a judicious use of normalisation factors. Thus we have reanalyzed those data seeking a better understanding of the structures of the exotic ions. To do so we have used the Melbourne g -folding model of scattering [1] together with a microscopic distorted wave approximation (DWA) to describe inelastic processes. The shell model has been used

to specify the putative structures of the ions.

II. STRUCTURE AND REACTION THEORY

In this section we give details of the structure of the exotic (RIB) nuclei and of the theories used to evaluate elastic and inelastic data from the scattering of those RIB nuclei from hydrogen.

A. Many nucleon structures of ${}^8\text{He}$, ${}^{10,11}\text{C}$, and ${}^{18,20,22}\text{O}$

${}^8\text{He}$ lies at the neutron drip line. It is weakly bound with a two-neutron separation energy of 2.137 MeV [11]. It is also an example of a Borromean nucleus as ${}^7\text{He}$ is unbound, as is any two-body subsystem of ${}^8\text{He}$. We have used a no-core shell model to define its ground state. That has been obtained in a complete $(0 + 2 + 4)\hbar\omega$ model space using the G -matrix interaction of Zheng *et al.* [12]. That ground state specification has been used previously in analyses of scattering data at 68A MeV [4].

Spectra for ${}^8\text{He}$ are given in Fig. 1. The $(0 + 2 + 4)\hbar\omega$ shell model results are compared

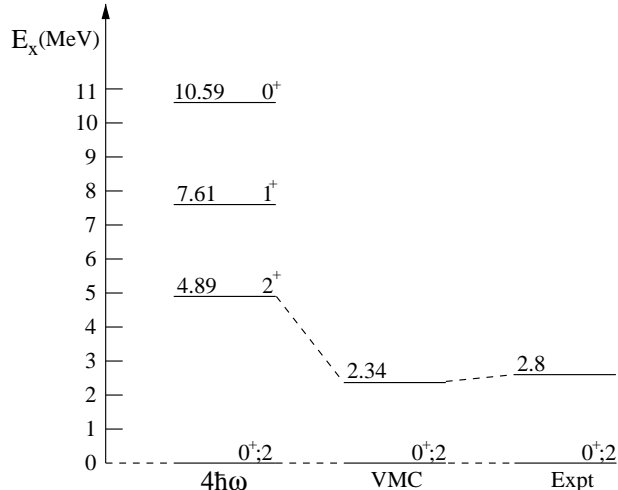


FIG. 1: The spectrum of ${}^8\text{He}$. The result of the $(0 + 2 + 4)\hbar\omega$ shell model calculation is compared with that of the VMC calculation [13].

not only with known data [14] but also with values determined by a variational Monte Carlo (VMC) calculation [14]. There is very little experimental information on the spectrum of ${}^8\text{He}$. The first excited state is listed at 2.8 ± 0.4 MeV and has $J^\pi; T = (2^+); 2$ [11]. Other states, at 1.3, 2.6, and 4.0 MeV [11], have been suggested from a heavy ion transfer experiment, but as yet no other data support their existence.

The results of the VMC calculation place the 2_1^+ state in very close agreement with experiment. However, that calculation places an extra 1^+ state in the spectrum. Not only has that state not been observed in experiment, but also it has not been found with other calculations. The shell model results clearly need improving to reduce the gap energy. Such suggest that an even larger space is required. However, binding energies reflect the asymptotic properties of wave functions and other tests are required to probe the credibility

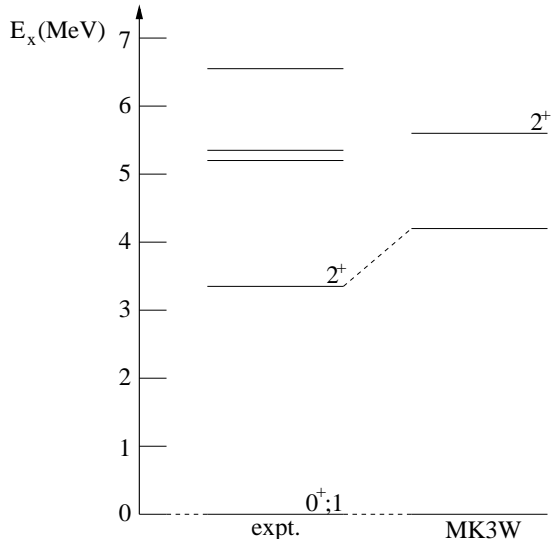


FIG. 2: Energy spectrum of ^{10}C . The result of the $(0 + 2)\hbar\omega$ calculation is compared to the data of Ref. [18].

of current wave functions through the nuclear medium. A first test is the root mean square (r.m.s.) radii, which is most sensitive to characteristics of the (outer) surface of a nucleus. Using our shell model gave an r.m.s. value for ^8He of 2.63 fm, which is in good agreement with the value of 2.6 fm extracted from high energy data using a cluster model [15].

Wave functions of ^{10}C and ^{11}C were obtained in a complete $(0 + 2)\hbar\omega$ model space using the MK3W interaction [16]. That model reproduced the ^{12}C spectrum to 20 MeV [17], with the exception of the superdeformed 0^+ state at 7.65 MeV. There is little known about the spectrum of ^{10}C as is shown in Fig. 2. The $2^+;1$ excited state is at 3.354 MeV [18] while the SM prediction puts it at 4.272 MeV. The state at 6.58 MeV has been given a tentative assignment of 2^+ for which the corresponding state in the SM spectrum lies at 5.613 MeV. There is no indication in the SM result of the two states below it. They have not been given assignments and may be intruder states.

The spectrum of ^{11}C is shown in Fig. 3. Therein, the results of $(0 + 2)\hbar\omega$ and $(1 + 3)\hbar\omega$ SM calculations, for negative and positive parity states respectively, are compared to the data [19]. There is better agreement with the known spectrum in this case.

The ground states for $^{18,20,22}\text{O}$ were obtained from a complete $0\hbar\omega$ SM calculation using the USD interaction of Brown and Wildenthal [20]. This model of structure suffices for use in describing the elastic scattering data from these nuclei. For the inelastic scattering to states in ^{20}O and ^{22}O , we also obtained the transition densities in this model, noting that there may be scaling of the cross sections due to core polarization corrections.

B. The g -folding optical potential for elastic scattering

A detailed study of the g -folding optical potential has been published [1] and so only salient features are presented. In coordinate space, that optical potential can be written as

$$U(\mathbf{r}, \mathbf{r}'; E) = \delta(\mathbf{r} - \mathbf{r}') \sum_i n_i \int \varphi_i^*(\mathbf{r}) g^D(\mathbf{r}, \mathbf{s}; E) \varphi_i(\mathbf{s}) ds + \sum_i n_i \varphi_i^*(\mathbf{r}) g^E(\mathbf{r}, \mathbf{r}'; E) \varphi_i(\mathbf{r}') \quad (1)$$

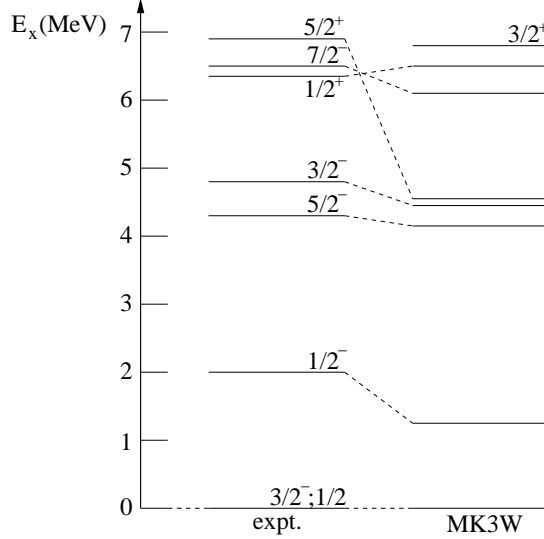


FIG. 3: Energy spectrum of ^{11}C . The results of the shell model calculations are compared to the data of Ref. [19].

To evaluate these potentials requires specification of three quantities. They are the single nucleon bound state wave functions $\varphi_i(\mathbf{r})$, the orbit occupancies n_i which, more properly are the nuclear state OBDME, and the NN g -matrices $g^{D/E}(\mathbf{r}, \mathbf{r}'; E)$. Those g -matrices are appropriate combinations of NN interactions in the nuclear medium for diverse NN angular momentum channels [1]. For the latter, much success has been had using effective NN interactions, now commonly designated as the Melbourne force, which have the form $g_{01}^{ST} \equiv g_{\text{eff}}^{ST}(r, E; k_f(R))$ where $r = |\mathbf{r}_0 - \mathbf{r}_1|$ and $R = \frac{1}{2}(\mathbf{r}_0 + \mathbf{r}_1)$. Therein the Fermi momenta relate to the local density in the nucleus at distance R from the center when \mathbf{r}_i are the coordinates of the colliding projectile and bound nucleons. $\{ST\}$ are the NN spin and isospin quantum numbers.

For use in the DWBA98 program, these effective NN g -matrices are, more specifically,

$$\begin{aligned}
 g_{\text{eff}}^{ST}(\mathbf{r}, E; k_f) &= \sum_{i=1}^3 \left[\sum_{j=1}^4 S_j^{(i)}(E; k_f) \frac{e^{-\mu_j^{(i)} r}}{r} \right]_{[S,T]} \Theta_i \\
 &= \sum_i g_{\text{eff}}^{(i)ST}(r, E; k_f) \Theta_i, \quad (2)
 \end{aligned}$$

where Θ_i are the characteristic operators for central forces ($i = 1$), $\{1, (\sigma \cdot \sigma), (\tau \cdot \tau), (\sigma \cdot \sigma \tau \cdot \tau)\}$, for the tensor force ($i = 2$), $\{\mathbf{S}_{12}\}$, and for the two-body spin-orbit force ($i = 3$), $\{\mathbf{L} \cdot \mathbf{S}\}$. The $S_j^{(i)}(E; k_f)$ are complex, energy- and density-dependent strengths. The properties of the g -matrices are such that the ranges of the Yukawa form factors, as assumed in the above, can be taken as independent of energy and density [1].

The strengths (and ranges) in these effective NN interactions were found by mapping the double Bessel transforms of them to the NN g -matrices in infinite nuclear matter that are solutions of the partial wave Bethe-Brueckner-Goldstone (BBG) equations [1]. With the

BBG g -matrices denoted by $g_{\text{BBG};LL'}^{JST}(q', q; E)$, the mapping is

$$\begin{aligned}
g_{\text{BBG};LL'}^{JST}(q', q; E) &= \sum_i \langle \theta_i \rangle \int_0^\infty r^{2+\lambda} j_{L'}(q'r) g_{\text{eff}}^{(i)ST}(r, E; k_f) j_L(qr) dr \\
&= \sum_{ij} \langle \theta_i \rangle S_j^{(i)}(\omega) \int_0^\infty r^{2+\lambda} j_{L'}(q'r) \frac{e^{-\mu_j^{(i)}r}}{r} j_L(qr) dr \\
&= \sum_{ij} \langle \theta_i \rangle S_j^{(i)}(\omega) \tau^\alpha(q', q; \mu_j^{(i)}) ,
\end{aligned} \tag{3}$$

where $\alpha : \{LL'JST\}$ and $\lambda = 0$ save for the tensor force for which it is 2. In application, a singular-valued decomposition has been used to effect this mapping and it was found that four Yukawa functions for the central force and four with other ranges for the spin-orbit and tensor forces sufficed to give close mapping to both on- and, a near range of, off-shell values of the BBG g -matrices in 32 NN S, T channels and for energies to 300 MeV.

The other requirements come from the assumed models of structure. The many-nucleon aspects, the OBDME, are the ground state reduced matrix elements of particle-hole operators

$$S_{jj0} = \left\langle \Psi_{g.s.} \left\| \left[a_j^\dagger \times \tilde{a}_j \right]^0 \right\| \Psi_{g.s.} \right\rangle , \tag{4}$$

and which are defined more generally in regard to transitions in the following subsection. If there are no non-Hartree-Fock contributions, these OBDME reduce to the shell occupancies in the ground state. The single nucleon (bound state) wave functions usually are chosen either to be harmonic oscillators with oscillator length as used in the shell model calculations or from a Wood-Saxon potential. The parameters of that Wood-Saxon potential are chosen to give wave function solutions that meet some criteria such as the r.m.s. radius or an electron scattering form factor.

C. The distorted wave approximation for inelastic scattering

In the DWA, amplitudes for inelastic scattering of nucleons through a scattering angle θ and between states J_i, M_i and J_f, M_f in a nucleus, are given by

$$\begin{aligned}
T_{J_f J_i}^{M_f M_i \nu' \nu}(\theta) &= \\
\left\langle \chi_{\nu'}^{(-)}(\mathbf{k}_o 0) \right| \left\langle \Psi_{J_f M_f}(1 \cdots A) \right| A \sum_{ST} g_{\text{eff}}^{ST}(r_{01}, E; k_f) P_S P_T \mathcal{A}_{01} \left\{ \left| \chi_{\nu}^{(+)}(\mathbf{k}_i 0) \right\rangle \left| \Psi_{J_i M_i}(1 \cdots A) \right\rangle \right\} ,
\end{aligned} \tag{5}$$

where ν, ν' are the spin quantum numbers of the nucleon in the continuum, $\chi^{(\pm)}$ are the distorted waves, and $g_{\text{eff}}^{ST}(r_{01}, E; k_f) P_S P_T$ is the spin-isospin Melbourne force. The operator \mathcal{A}_{01} effects antisymmetrization of the two-nucleon product states.

Then, by using cofactor expansions of the nuclear states, i.e.

$$|\Psi_{JM}\rangle = \frac{1}{\sqrt{A}} \sum_{j,m} |\varphi_{jm}(1)\rangle a_{jm} |\Psi_{JM}\rangle , \tag{6}$$

the matrix elements become

$$T_{J_f J_i}^{M_f M_i \nu \nu'}(\theta) = \sum_{j_1 j_2 S T} \left\langle J_f M_f \left| a_{j_2 m_2}^\dagger a_{j_1 m_1} \right| J_i M_i \right\rangle \\ \times \left\langle \chi_{\nu'}^{(-)}(\mathbf{k}_o 0) \left| \langle \varphi_{j_2 m_2}(1) | g_{\text{eff}}^{ST}(r_{01}, E; k_f) P_S P_T \mathcal{A}_{01} \{ |\chi_{\nu}^{(+)}(\mathbf{k}_i 0) \rangle | \varphi_{j_1 m_1}(1) \rangle \} \right. \right\rangle . \quad (7)$$

The density matrix elements in the amplitudes reduce as

$$\left\langle J_f M_f \left| a_{j_2 m_2}^\dagger \times a_{j_1 m_1} \right| J_i M_i \right\rangle \\ = \sum_{I(N)} (-1)^{j_1 - m_1} \langle j_1 m_1 j_2 - m_2 | I N \rangle \left\langle J_f M_f \left| \left[a_{j_2}^\dagger \times \tilde{a}_{j_1} \right]^{IN} \right| J_i M_i \right\rangle \\ = \sum_{I(N)} \frac{(-1)^{j_1 - m_1}}{\sqrt{2J_f + 1}} \langle j_1 m_1 j_2 - m_2 | I N \rangle \langle J_i M_i I N | J_f M_f \rangle S_{j_1 j_2 I} , \quad (8)$$

where $S_{j_1 j_2 I}$ are the transition OBDME. The DWA amplitudes are then (with $\xi = \{j_1, j_2, m_1, m_2, I(N), S, T\}$)

$$T_{J_f J_i}^{M_f M_i \nu \nu'}(\theta) = \sum_{\xi} \frac{(-1)^{j_1 - m_1}}{\sqrt{2J_f + 1}} S_{j_1 j_2 I} \langle j_1 m_1 j_2 - m_2 | I N \rangle \langle J_i M_i I N | J_f M_f \rangle \\ \times \left\langle \chi_{\nu'}^{(-)}(\mathbf{k}_o 0) \left| \langle \varphi_{j_2 m_2}(1) | g_{\text{eff}}^{ST}(r_{01}, E; k_f) P_S P_T \mathcal{A}_{01} \{ |\chi_{\nu}^{(+)}(\mathbf{k}_i 0) \rangle | \varphi_{j_1 m_1}(1) \rangle \} \right. \right\rangle . \quad (9)$$

In our calculations of these DWA amplitudes, a) the g -folding model has been used to determine the distorted waves in both the incident and emergent channels, b) the same effective NN interaction has been used as the transition operator, c) shell models have been used to find the transition OBDME, and d) the single nucleon wave functions chosen to form the optical potentials have also been used for the single nucleon states.

III. RESULTS

In previous papers [5, 21], the cross sections from the elastic and inelastic scattering (to the 2_1^+ state) of $40.9A$ and $24.5A$ MeV ${}^6\text{He}$ ions from hydrogen were analyzed using the methods described above. Those results provided clear evidence that ${}^6\text{He}$ had an extended neutron matter distribution consistent with a neutron halo. Similar analyses of elastic scattering data from the scattering of $72A$ MeV ${}^8\text{He}$ ions from hydrogen suggested that it had a neutron skin but not the extended distribution of a halo [4]. Recently [6] data from the scattering of $15.7A$ MeV ${}^8\text{He}$ ions from hydrogen has been reported, and we consider that now. The energy is the smallest at which the g -folding method has been applied. In most nuclei in the excitation energy range ~ 10 to ~ 30 MeV there are giant resonances; the coupling to which is known [22] to influence nucleon scattering. When that is so, corrections to the g -folding premise need be made. However, an important exception is the set of Helium isotopes for which there are no giant resonances. With ${}^8\text{He}$ also, the nucleon break-up threshold lies at just a few MeV so that 15 MeV is well in the continuum of the nucleus. For these reasons, it should be appropriate to use the g -folding approach to analyze the 15.7A MeV data.

A. The elastic scattering of $15.7A$ MeV ${}^8\text{He}$ from hydrogen

Using the structure of the ground state described previously and with the 15 MeV Melbourne force, two predictions of the $15.7A$ MeV ${}^8\text{He}$ - p scattering have been made. The results are compared with the data in Fig. 4. The result shown by the dashed curve was

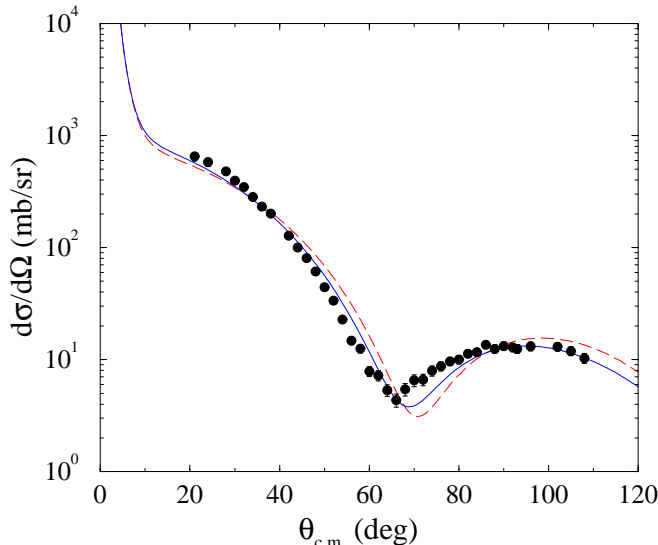


FIG. 4: (Color online) Differential cross sections for the elastic scattering of $15.7A$ MeV ${}^8\text{He}$ ions from hydrogen. The data [6] are compared with g -folding model results. The curves are identified in the text.

found by using oscillator wave functions for the single nucleon states in the folding process, while that shown by the solid curve was found using Woods-Saxon functions generated with the potential used before [5, 21]. Clearly the predictions are in very good agreement with this data with preference (as was found before) for the Woods-Saxon single-nucleon wave function set. The JLM model results [6] do better in reproducing this data around 80° but do not as well at forward scattering angles. However, the JLM results required some *a posteriori* adjustment of the real and imaginary strengths of the optical potential from those considered standard. That, and the strength of the measured ${}^8\text{He}(p, d)$ cross section, led them to believe that a second order $(p, d)(d, p)$ process was important in the description of elastic scattering. But, the measurement of the (p, d) reaction was inclusive with no identification of the final state being ${}^7\text{He}$. As ${}^7\text{He}$ is unbound against neutron emission there are many multi-particle exit channels from the (p, d) reaction and the likelihood of the conglomerate reforming to a ${}^8\text{He}$ and proton is very small. In fact the plethora of propagating channels (given the energy and momentum sharing possible) is one reason why an optical potential approach is appropriate.

B. The scattering of ${}^{10,11}\text{C}$ ions from hydrogen

Another GANIL experiment [8] determined differential cross sections for the elastic and inelastic scattering of $45.3A$ MeV ${}^{10}\text{C}$ ions and of $40.6A$ MeV ${}^{11}\text{C}$ ions from hydrogen. That data are compared with predictions in Figs. 5 and 6. Previously, data taken at $40.9A$

MeV [5, 21] of ${}^6\text{He}$ ions elastically and inelastically scattered from hydrogen were predicted well with the g -folding method. The current results, with which the new data are compared in these two figures, were found by using the structure as described earlier. Also we have used the same Melbourne force that was used in the analyses of the ${}^6\text{He}$ data [5, 21] and either oscillator or Woods-Saxon wave functions for the bound nucleons. Note that in these

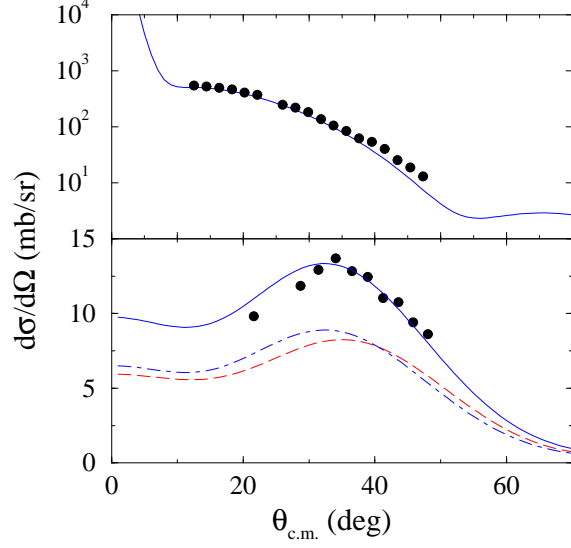


FIG. 5: (Color online) Differential cross sections for the elastic (top) and inelastic scattering to the 2_1^+ state (bottom) of $45.3A$ MeV ${}^{10}\text{C}$ ions from hydrogen.

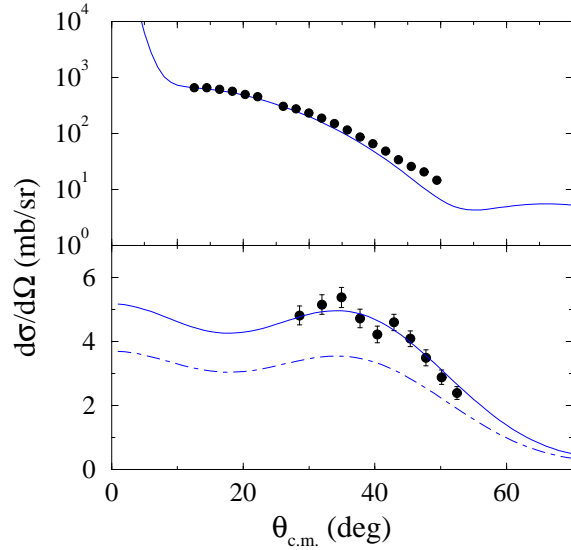


FIG. 6: (Color online) Differential cross sections for the elastic (top) and inelastic scattering to the $\frac{5}{2}^-$ state (bottom) of $40.6A$ MeV ${}^{11}\text{C}$ ions from hydrogen.

diagrams the inelastic scattering data and results are plotted on a linear scale to emphasize any shortfalls.

In Fig. 5, cross sections for the scattering of ^{10}C are shown. Clearly the elastic scattering prediction agrees with the data almost as well as the phenomenological JLM analyses of Jouanne *et al.* [8]. With the inelastic scattering (to the 2^+ ; 3.36 MeV state), the results found using the OBDME from the shell model calculations described before and with oscillator (dashed) and Woods-Saxon (dot-dashed) functions for the single-nucleon states required in the DWA calculations lie below the data values. A scaling of 1.5 on the Woods-Saxon result gives the solid curve which is in very good agreement with the data. Scaling was also required with the phenomenological model analyses [8]. In our case, however, given the propriety (admittedly mostly justified through numerous uses) of

1. the model, and in particular with it, specific treatment of the exchange amplitudes;
2. the transition operator (Melbourne force) in which account is taken of medium effects on the NN interaction; and
3. the single-nucleon wave functions which link well to ground state properties;

the shortfall we attribute to a limitation of the many-nucleon structure for the ion itself. It has been long known [1] that core polarization corrections, be they made phenomenologically or by appropriate increase in the space in which the structure is assessed, influence inelastic scattering evaluations strongly; and most obviously when collective enhancing excitations are involved. That the amount in the case of ^{10}C is but a 50% enlargement attests to the reasonable first guess that is given by the structure calculations made using the MK3W potentials. The enlargement equates to a polarization charge, $\Delta e \approx 0.11e$.

In Fig. 6, the 40.6A MeV ^{11}C results are shown. The elastic scattering data are again well predicted by the g -folding method. Likewise the cross section for excitation of the $\frac{5}{2}^-$; 4.32 MeV state as predicted using Woods-Saxon wave functions (dot-dashed curve) reproduces the observed data very well when a small upward scale (of 1.4) is made.

Thus the MK3W structure adopted for these states in $^{10,11}\text{C}$ is quite good. Use of that structure in the scattering calculations gave cross-section shapes very like that observed in the data and requiring but a small amount of core polarization to reproduce the measured data from the inelastic ($E2$ dominant) transitions. We surmise that the first complete basis space enlargement possible to the shell model scheme we have used to describe these nuclei will give much, if not all, of such enhancement.

C. The $^{18,20,22}\text{O}$ isotopes

Recently the cross sections from 43A MeV $^{18,20}\text{O}$ ions and from 46.6A MeV ^{22}O ions scattering from hydrogen targets have been measured [9, 10]. Cross sections for both the elastic and the inelastic excitation of 2_1^+ states of those ions were obtained. Those data are shown in the top, middle, and bottom panels of Fig. 7. Those data are compared with our predictions (g -folding for the elastic and DWA for the inelastic transitions) built with the $0\hbar\omega$ shell model wave functions and the Melbourne force. The elastic scattering cross-section predictions depicted by the solid lines agree well with the data (filled circles) save that the $^{18,20}\text{O}$ results have an over-pronounced minimum near 40° . The inelastic scattering cross sections given by our approach are those depicted by the long dashed curves and they all are smaller than any of the data sets (opaque circles). The solid curves that match the inelastic data well are those calculated values increase by factors of 2 (^{18}O), 5 (^{20}O), and

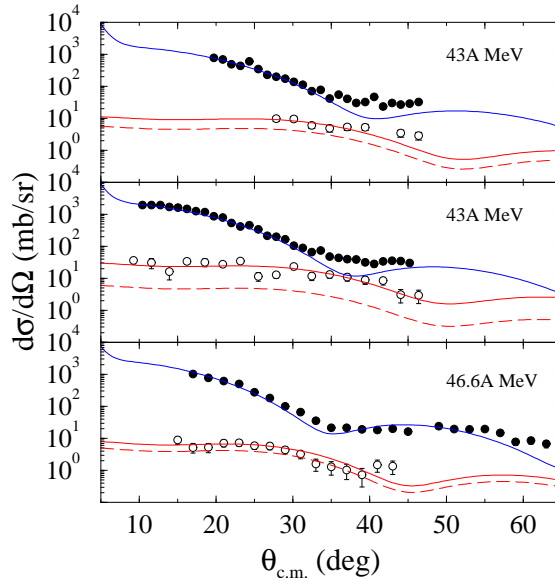


FIG. 7: (Color online) Differential cross sections for the elastic and inelastic scattering (to the 2_1^+ states) with the isotopes of oxygen, top (^{18}O), middle (^{20}O), and bottom (^{22}O). The energies are as indicated.

1.6 (^{22}O). These ratios are quite similar to those of the squares of the deformations required in a previous analysis of this data [23]. That analysis also found very good fits to all of the elastic scattering data, but to do so involved using many parameters including separate renormalization of the real and imaginary components of the optical potentials, and for each nucleus independently.

With our results for the inelastic scattering cross sections one can envisage different degrees of core polarization being required with the base valence models having 2, 4, and 6 (full sub-shell) $d_{5/2}$ -orbit occupancies as the dominant term in the description of the ground states of $^{18,20,22}\text{O}$ respectively. That ^{20}O requires largest scaling is reflective of that nucleus having considerably more configuration mixing than the other isotopes in a good description of its states.

IV. CONCLUSIONS

The microscopic g -folding approach to analysis of data from the elastic scattering of radioactive ion beams from hydrogen targets when the beam energy equates to an excitation of those ions sufficiently in their continua, is most appropriate. When essentials are satisfied, that approach can, and does, give predictions of elastic scattering that one may have confidence in being a good representation of observation. It is essential, though, to use a realistic energy- and medium-dependent effective NN interaction in the folding. Also it is essential that as good a prescription as possible be made for the distributions of nucleons in the ground state of the ion. Finally one must be faithful to the Pauli principle, not only in the specification of the effective NN interaction, but also in the calculation of the scattering allowing for the knock-out process. Doing so introduces a specific non-local term in the optical potential. Our experience is that such non-locality should be treated as exactly as

possible and not localized to simplify the problem to solution of a set of local Schrödinger equations.

We have also shown that the DWA suffices to analyze the inelastic scattering cross sections. There is a proviso that the energy is sufficient that coupled-channel effects due to discrete and/or giant resonance states of the ion are not important. When such is not the case, other methods of analysis, such as with a multichannel algebraic scattering theory [24], are more relevant. Even then it has been noted that due care of the Pauli principle is essential [25]. But for data at the energies considered, the DWA worked very well. With all details preset, the DWA results are also predictions which, in the cases considered, well reproduced the shapes of the data. All of those calculated results had to be enhanced to meet the magnitudes of that data but those scalings were consistent with the core polarization one must expect for shell model wave functions defined in the small bases we have used.

-
- [1] K. Amos, P. J. Dortmans, H. V. von Geramb, S. Karataglidis, and J. Raynal, *Adv. Nucl. Phys.* **25**, 275 (2000).
 - [2] *Technical Proposal for the Design, Construction, Commissioning, and Operation of the ELISE setup*, spokesperson Haik Simon, GSI Internal Report, Dec. 2005.
 - [3] T. Suda and M. Wakasugi, *Prog. Part. Nucl. Phys.* **55**, 417 (2005).
 - [4] S. Karataglidis, P. J. Dortmans, K. Amos, and C. Bennhold, *Phys. Rev. C* **61**, 024319 (2000).
 - [5] A. Lagoyannis et al., *Phys. Lett.* **B518**, 27 (2001).
 - [6] F. Skaza et al., *Phys. Rev. C* **72**, 014308 (2005).
 - [7] P. Navrátil and B. R. Barrett, *Phys. Rev. C* **57**, 3119 (1998).
 - [8] C. Jouanne et al., *Phys. Rev. C* **72**, 014308 (2005).
 - [9] E. Becheva et al., *Phys. Rev. Lett.* **96**, 012501 (2006).
 - [10] E. Khan et al., *Phys. Lett.* **B490**, 45 (2000).
 - [11] F. Ajzenberg-Selove, *Nucl. Phys.* **A490**, 1 (1988).
 - [12] D. C. Zheng, B. R. Barrett, J. P. Vary, W. C. Haxton, and C. L. Song, *Phys. Rev. C* **52**, 2488 (1995).
 - [13] R. B. Wiringa, *Nucl. Phys.* **A631**, 70c (1998).
 - [14] B. S. Pudliner, V. R. Pandharipande, J. Carlson, S. C. Piper, and R. B. Wiringa, *Phys. Rev. C* **56**, 1720 (1997).
 - [15] J. S. Al-Khalili and J. A. Tostevin, *Phys. Rev. C* **57**, 1846 (1998).
 - [16] E. K. Warburton and D. K. Millener, *Phys. Rev. C* **39**, 1120 (1989).
 - [17] S. Karataglidis, P. J. Dortmans, K. Amos, and R. de Swiniarski, *Phys. Rev. C* **52**, 861 (1995).
 - [18] D. R. Tilley, J. H. Kelley, J. L. Godwin, D. J. Millener, J. E. Purcell, C. G. Sheu, and H. R. Weller, *Nucl. Phys.* **A745**, 155 (2004).
 - [19] F. Ajzenburg-Selove, *Nucl. Phys.* **A506**, 1 (1990).
 - [20] B. A. Brown and B. H. Wildenthal, *Ann. Rev. Nucl. Part. Sci.* **36**, 29 (1988).
 - [21] S. V. Stepantsov et al., *Phys. Lett.* **B542**, 35 (2002).
 - [22] H. V. von Geramb, K. Amos, R. Sprickmann, K. T. Knöpfle, M. Rogge, D. Ingham, and C. Mayer-Böricke, *Phys. Rev. C* **12**, 1697 (1975).
 - [23] D. Gupta, E. Khan, and Y. Blumenfeld, *Nucl. Phys.* **A773**, 230 (2006).
 - [24] L. Canton, G. Pisent, J. P. Svenne, K. Amos, and S. Karataglidis, *Phys. Rev. Lett.* **96**, 072502 (2006).

- [25] K. Amos, S. Karataglidis, D. van der Knijff, L. Canton, G. Pisent, and J. P. Svenne, Phys. Rev. C **72**, 064604 (2005).